JOURNAL OF THERMOPHYSICS AND HEAT TRANSFER
Vol. 8, No. 3, July–Sept. 1994

Effective Radiative Properties of Fibrous Composites Containing Spherical Particles

Siu-Chun Lee*
Applied Sciences Laboratory, Inc., Hacienda Heights, California 91745
Susan White†
NASA Ames Research Center, Moffett Field, California 94035
and
Jan A. Grzesik‡
Applied Sciences Laboratory, Inc., Hacienda Heights, California 91745

The influence of spherical particles on the radiative properties of high-porosity fibrous composites is examined in this article. The radiative properties formulation is based on the independent scattering assumption, which utilizes the solution of Maxwell's equations for the interaction of electromagnetic waves with the respective types of particles. The extinction, absorption, and scattering coefficients, as well as the scattering phase function of the composites are formulated as the weighted average according to the fractional volume of the constituent particulates. The models are applied to predict the radiative properties of thermal insulation composites containing fibers and spheres that are made of zirconia and silica. Numerical results are presented to illustrate the influence of the respective types of particulates on the radiative properties of the composites.

Nomenclature

f_v = solid volume fraction
$i_{s\lambda}$ = scattered intensity function of spheres
$K_{e\lambda}$ = extinction coefficient
k = absorption index
m = complex index of refraction, $n - ik$, $i = \sqrt{-1}$
n = refractive index or summation index
$\bar{P}_\lambda$ = effective phase function of composite
$p_{f\lambda}$ = phase function of fibers
$p_{s\lambda}$ = phase function of spheres
$Q_{f,e\lambda}$ = extinction efficiency of fibers
$Q_{f,s\lambda}$ = scattering efficiency of fibers
$Q_{s,e\lambda}$ = extinction efficiency of spheres
$Q_{s,s\lambda}$ = scattering efficiency of spheres
r = radius of sphere or fiber
x_f = fraction of fiber by volume
α = size parameter, $2\pi r/\lambda$
Θ = scattering angle
θ = angle of observation for fibers
λ = wavelength
μ, μ' = cosine of polar angle, cos ξ
ξ = polar angle
π_n = Legendre polynomial function
σ_s = scattering coefficient
τ_n = Legendre polynomial function
ϕ = angle of incidence on a fiber
ϕ_c = complementary angle of incidence on a fiber, $\pi/2 - \phi$
Ω = dummy coefficient in Eq. (17)
ω = azimuthal angle

Subscripts
f = fibers
s = spheres
λ = wavelength

Superscript
r = random orientation

Presented as Paper 93-2729 at the AIAA 28th Thermophysics Conference, Orlando, FL, July 6–9, 1993; received July 26, 1993; revision received Nov. 29, 1993; accepted for publication Dec. 1, 1993.

*Vice President. Member AIAA.
†Research Scientist. Member AIAA.
‡Senior Scientist.

Introduction

DEVELOPMENT of advanced thermal protection materials has long been recognized as a key technology issue to the success of future aerospace systems. Spacecraft of future missions are expected to encounter substantially higher temperatures and heat fluxes than those of the present missions. In particular, uv radiation from the shock layer is expected to constitute a significant portion of surface heat transfer to aerobraking atmospheric re-entry vehicles.[1–3] When radiative energy dominates the heat flux to atmospheric re-entry vehicles, an effective thermal control strategy is to reduce the amount of absorbed radiation by reflecting a large fraction of the irradiation. For example, Howe and Yang[4] investigated the use of highly backscattering ablating composites for high radiation re-entry trajectories. Stewart et al.[5] and White[6] examined the use of reflective coatings. Leiser et al.[7] incorporated strongly absorbing and emitting particles into a ceramic insulation to achieve higher insulation performance.

The continual increase in system complexity and operational constraints underlines the critical need for new thermal insulation materials that can perform over a wide range of temperatures and heat fluxes. A novel, effective thermal insulation to accommodate these requirements can be achieved by combining the high-temperature resistant properties of fibrous materials with the reflective characteristics of spherical particles. This type of insulation materials can be fabricated by dispersing spherical particles into a fibrous composite. By selecting the material and size of the fibers and spheres, the radiative behavior of the fiber-sphere composite can be en-

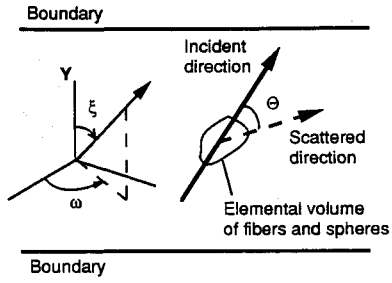

Fig. 1 Geometric configuration of the scattering directions.

gineered to exhibit spectrally selective reflective properties tailored to a given set of thermal environments.

Successful development of the fiber-sphere thermal insulation composite requires both modeling and experimentation in order to optimize the design. Analytical models must first be developed to evaluate the influence of the constituent particulates on the thermal radiative properties of the composite. Although the thermal insulation capacity of any given material can be measured, the large number of design parameters, which include the size, spectral optical properties, and particulate mixture fraction, would require the compilation of a large data base in order to determine the influence of the various parameters.

To fabricate and perform tests on enough samples to encompass all combinations of the design variables obviously presents a formidable task. A more cost-effective design approach is to perform numerical analyses by utilizing mathematical models that are based on fundamental principles. An optimal design can then be achieved in an efficient manner by conducting numerical analyses before producing a limited number of optimized material samples for experimental verification. The objective of this article is to present analytical models for the radiative properties of fiber-sphere composites, which can be used to guide the development of this type of thermal insulation materials.

Radiative Properties Modeling

The present study considers high-porosity composites (volume fraction less than 5%) which contain a mixture of fibers and spheres. In this case independent scattering is an adequate assumption because the average separation between the particles is sufficiently large relative to the particle size and wavelength of the incident radiation. The radiative properties of the medium can, therefore, be obtained by summing up the contributions of all the particles in the medium. For a composite containing both fibers and spheres, the effective radiative properties of the composite are obtained by weighting the properties of the respective types of scatterers by their solid volume fraction. The radiative properties of fibers and spheres are based on rigorous solutions of Maxwell's equations for the interaction of electromagnetic (EM) radiation with an isolated infinite cylinder and sphere whose diameters are comparable to the wavelength.[8,9] The fibers are modeled as infinite cylinders because the typical length of fibers in Space Shuttle tile materials is much greater than the wavelength of thermal radiation. The effective radiative properties of a fibrous medium have been shown to be strongly dependent on the orientation of fibers.[10-12]

The properties which govern the thermal performance of a composite include the radiative coefficients and the scattering phase function. The extinction and scattering coefficients for a high-porosity medium of monosize spheres are given by

$$K_{s,e\lambda}(\alpha_s, m) = (3f_v/4r_s)Q_{s,e\lambda} \tag{1}$$

$$\sigma_{s,s\lambda}(\alpha_s, m) = (3f_v/4r_s)Q_{s,s\lambda} \tag{2}$$

respectively, where r_s is the radius of sphere. The extinction and scattering efficiencies $Q_{s,e\lambda}$ and $Q_{s,s\lambda}$ are given by the Mie theory.[8,9] The absorption coefficient $\sigma_{a\lambda}$ is equal to the difference between the extinction and scattering coefficients.

The phase function for an isolated sphere is defined as the angular distribution of the scattered radiation normalized by its directional average. For a spherical particle subjected to unpolarized radiation, the scattered intensity function is calculated as the average of the two polarized components[8,9]

$$i_{s\lambda}(\Theta) = 0.5\left\{\left|\sum_{n=1}^{\infty}\frac{2n+1}{n(n+1)}[a_n\pi_n(\cos\Theta) + b_n\tau_n(\cos\Theta)]\right|^2 + \left|\sum_{n=1}^{\infty}\frac{2n+1}{n(n+1)}[b_n\pi_n(\cos\Theta) + a_n\tau_n(\cos\Theta)]\right|^2\right\} \tag{3}$$

where a_n and b_n are given in terms of spherical Bessel and Hankel functions, and Θ is the angle between the incident and scattered radiation, as shown in Fig. 1. The functions π_n and τ_n are expressed in terms of the Legendre polynomials. The phase function for an isolated sphere is given by

$$p_{s\lambda}(\Theta) = \frac{4i_{s\lambda}(\Theta)}{\alpha_s^2 Q_{s,s\lambda}} \tag{4}$$

which is a function of the size parameter α_s and optical properties m. The subscript λ in all of the above quantities is retained to emphasize that these quantities are wavelength-dependent.

In order to apply the single particle phase function to radiative transfer analysis through a planar medium, the angular dependence of the phase function must be transformed to the polar coordinates (ξ, ω) of a plane-parallel slab, as shown in Fig. 1. Since diffuse radiation independent of the azimuthal angle is considered, the phase function can be simplified by integrating over the azimuthal angle as

$$p_{s\lambda}(\mu, \mu') = \frac{1}{2\pi}\int_0^{2\pi} p_{s\lambda}(\Theta)\, d\omega \tag{5}$$

where $\mu = \cos\xi$. Using the relationship between Θ and the polar coordinates of the slab given by

$$\cos\Theta = \mu\mu' + \sqrt{(1-\mu^2)(1-\mu'^2)}\cos(\omega - \omega') \tag{6}$$

the phase function for a slab geometry becomes

$$p_{s\lambda}(\mu, \mu') = \frac{4}{\pi\alpha_s^2 Q_{s,s\lambda}} \times \int_{\Theta_1}^{\Theta_2}\frac{i_{s\lambda}(\Theta)\sin\Theta\, d\Theta}{\sqrt{(1-\mu^2)(1-\mu'^2) - (\cos\Theta - \mu\mu')^2}} \tag{7}$$

where the limits of integration are given by

$$\cos\Theta_1 = \mu\mu' + \sqrt{(1-\mu^2)(1-\mu'^2)} \tag{8}$$

$$\cos\Theta_2 = \mu\mu' - \sqrt{(1-\mu^2)(1-\mu'^2)} \tag{9}$$

Equation (7) is usually evaluated numerically to obtain the phase function for any particle size parameter.

For randomly-oriented fibers, the effective extinction and

scattering coefficients for an elemental volume of fibers are independent of incident angle. They are given by[11]

$$K_{f,e\lambda}(\alpha_f, m) = \frac{2f_v}{\pi r_f} Q^r_{f,e\lambda} = \frac{2f_v}{\pi r_f}\int_0^{\pi/2} Q_{f,e\lambda}(\phi)\cos\phi\, d\phi \quad (10)$$

$$\sigma_{f,s\lambda}(\alpha_f, m) = \frac{2f_v}{\pi r_f} Q^r_{f,s\lambda} = \frac{2f_v}{\pi r_f}\int_0^{\pi/2} Q_{f,s\lambda}(\phi)\cos\phi\, d\phi \quad (11)$$

respectively, where the superscript r denotes random orientation in space. The extinction and scattering efficiencies of fibers for general oblique incidence are summarized in Kerker.[9]

The scattering phase function for a fibrous medium with fibers in any prescribed orientation has been derived by Lee.[12] For a medium of monosize fibers randomly oriented in space, the phase function is given by

$$p_{f\lambda}(\Theta) = \frac{4}{\pi\alpha_f Q^r_{f,s\lambda}}\int_0^{\pi/2} \frac{i_{f\lambda}(\Theta, \phi_c)}{\sin\theta\sin^2\phi_c}\sin\phi_c\, d\phi_c \quad (12)$$

where $\phi_c(=\pi/2-\phi)$ is the complementary incident angle. The scattering angle Θ, which is the angle between the incident and scattered directions, is related to the angles ϕ and θ with respect to an isolated fiber by

$$\cos\theta = (\cos\Theta - \cos^2\phi_c)/\sin^2\phi_c \quad (13)$$

The phase function for a medium of randomly oriented fibers is then transformed into

$$p_{f\lambda}(\Theta) = \frac{4}{\pi\alpha_f Q^r_{f,s\lambda}} \times \int_0^1 \frac{i_{f\lambda}(\Theta, \phi_c)}{\sqrt{(1-\cos\Theta)(1+\cos\Theta-2\cos^2\phi_c)}}\, d(\cos\phi_c) \quad (14)$$

To apply this phase function in radiative transfer analyses through a slab, it must be expanded in terms of the coordinates of the slab. For diffuse boundary conditions, the radiative intensity is azimuthally independent. The slab fiber phase function can be obtained by integrating Eq. (14) over the azimuthal angles. Upon applying appropriate coordinate transformations, it is given by

$$p_{f\lambda}(\mu, \mu') = \frac{4}{\pi^2\alpha_f Q^r_{f,s\lambda}}\int_{\Theta_1}^{\Theta_2} \times \frac{\sin\Theta}{\sqrt{(1-\mu^2)(1-\mu'^2)-(\cos\Theta-\mu\mu')^2}} \times \int_0^1 \frac{i_{f\lambda}(\Theta, \phi_c)\, d(\cos\phi_c)}{\sqrt{(1-\cos\Theta)(1+\cos\Theta-2\cos^2\phi_c)}}\, d\Theta \quad (15)$$

In the present study the solid volume fraction is less than 5%, which is typical of ceramic fibrous insulations used on re-entry vehicles. The relatively low volume fraction is used in order to achieve minimal vehicle weight at launch. Based on the studies by Brewster and Tien[13] on spheres, and Lee[14] on fibrous medium, radiative energy transport through the high-porosity composite can be modeled by assuming independent scattering. The independent scattering assumption greatly simplifies the analysis of radiative energy transport through a particulate medium, because the radiative properties of the medium can be modeled as the sum of those of the individual particles. The effective radiative properties of the composite then follow as

$$\Omega = x_f\Omega_f + (1-x_f)\Omega_s \quad (16)$$

where Ω refers to the extinction $K_{e\lambda}$, absorption $\sigma_{a\lambda}$, and scattering $\sigma_{s\lambda}$ coefficients.

Because the phase function describes the distribution of scattered radiation for a given scattering coefficient, the phase function and the scattering coefficient must be considered as a group. Therefore, the scattering phase function of the composite is defined as

$$\sigma_{s\lambda}p_\lambda(\mu, \mu') = x_f\sigma_{f,s\lambda}p_{f\lambda}(\mu, \mu') + (1-x_f)\sigma_{s,s\lambda}p_{s\lambda}(\mu, \mu') \quad (17)$$

For the convenience of application in the radiative equation of transfer, we define the modified phase function as

$$\bar{P}_\lambda(\mu, \mu') = \sigma_{s\lambda}p_\lambda(\mu, \mu')/K_{e\lambda} \quad (18)$$

which is equivalent to the product of the scattering albedo and the conventional phase function.

Results

In this section the influence of composition, size, and materials on the radiative properties of the fiber-sphere composites is investigated. The objective of the present study is to evaluate the feasibility of engineering the composite to exhibit a high uv surface reflectance, while increasing the infrared emittance. The design parameters are chosen to guide the development of specific composites. Specifically, we examine two composites consisting of an equal proportion of fibers and spheres, i.e., $x_f = 0.5$, with one containing zirconia fibers and spheres, and the other silica fibers and spheres. The spectral optical properties of zirconia[15] are summarized in Table 1, and for silica[16] in Table 2. The radii of the zirconia fibers and spheres are 0.7 and 0.075 μm, respectively, whereas the radii of the silica fibers and spheres are both 1.5 μm. The numerical results presented below show the spectral variation of the phase function, the extinction and absorption coefficients, and the single scattering albedo. The influence of these properties on the radiative behavior is discussed in Ref. 17.

The modified scattering phase functions of the zirconia composite at 0.7 and 2.0 μm are shown in Figs. 2 and 3, respectively. The incident directions corresponding to the ordinates of a 20 point Gaussian quadrature. These phase functions display the general trend of a strong peak in the incident direction. The forward scattering peaks are particularly pronounced in the near normal directions, while they diminish as the incident direction approaches the horizon ($\mu = 0$). The magnitudes of the modified phase functions are similar for the two wavelengths, even though the size parameters differ

Table 1 Index of refraction of zirconia, $m = n - ik$

Wavelength, μm	n	k
0.3	1.96	1.244e-2
0.5	1.86	2.69e-3
0.7	1.86	2.05e-3
1.0	1.86	3.56e-3
2.0	1.92	4.0e-2

Table 2 Index of refraction of silica, $m = n - ik$

Wavelength, μm	n	k
0.25	1.51	6.9e-8
1.0	1.45	1.e-8
2.0	1.44	3.2e-7
4.0	1.395	5.79e-5
6.0	1.278	6.32e-3
8.0	0.4113	0.323
10.0	2.694	0.509
12.05	1.615	0.267

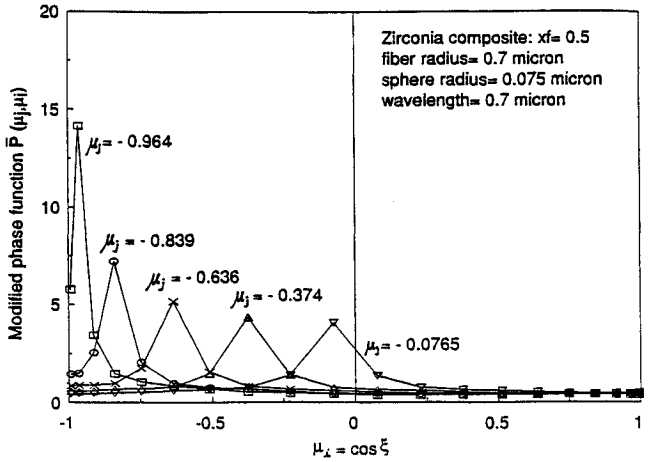

Fig. 2 Phase function of the zirconia composite at $\lambda = 0.7$ μm.

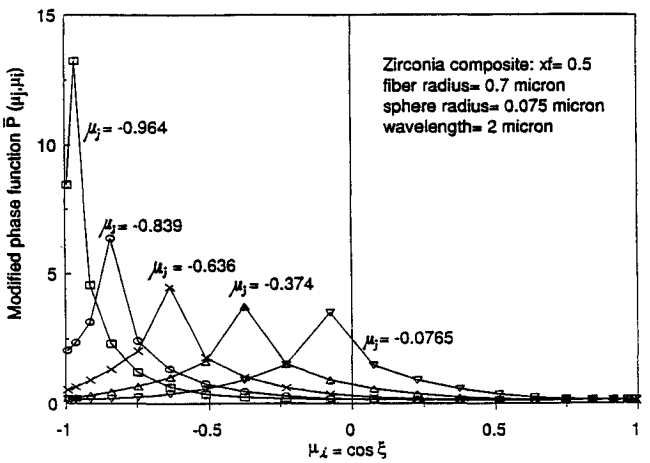

Fig. 3 Phase function of the zirconia composite at $\lambda = 2$ μm.

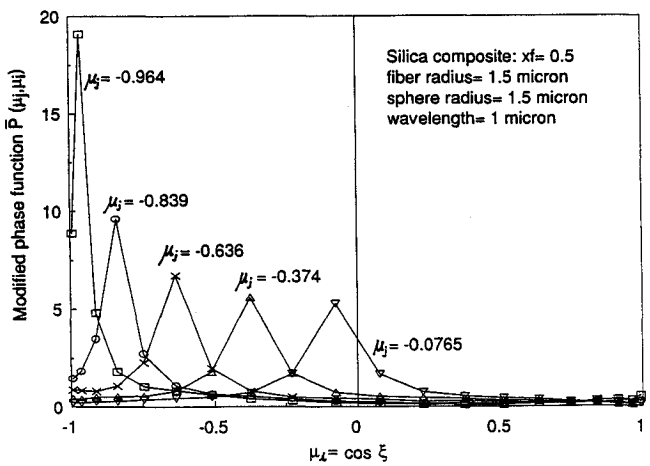

Fig. 4 Phase function of the silica composite at $\lambda = 1$ μm.

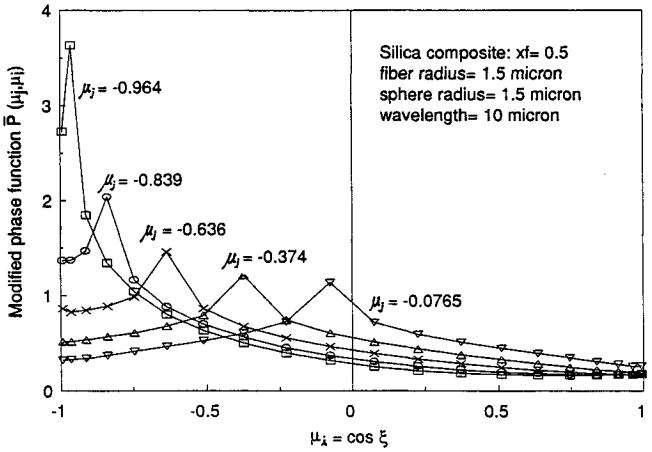

Fig. 5 Phase function of the silica composite at $\lambda = 10$ μm.

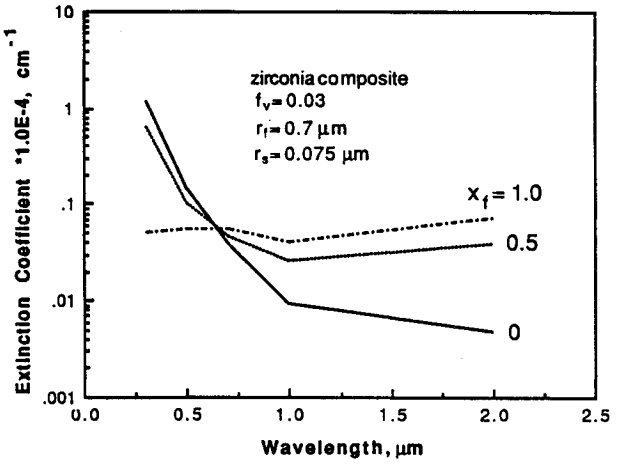

Fig. 6 Extinction coefficient of the zirconia composite for several fiber mixture fractions.

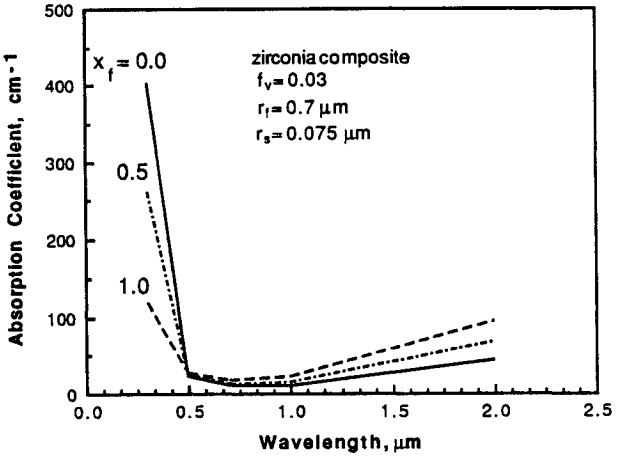

Fig. 7 Absorption coefficient of the zirconia composite for several fiber mixture fractions.

by a factor of 3. The small difference between the phase functions can be attributed to the almost identical index of refraction of zirconia at $\lambda = 0.7$ and 2 μm. The modified phase functions of the silica composite are shown in Figs. 4 and 5 at $\lambda = 1$ and 10 μm, respectively. The absorption index of silica is about 1.0e-8 at $\lambda = 1$ μm, while it is 0.509 at $\lambda = 10$ μm. The substantial absorption index at the latter wavelength results in much reduced forward scattering peaks at all incident angles compared to those at the shorter wavelengths where absorption is small. These results indicate that the common practice of employing a single phase function, such as the anisotropic or linear anisotropic forms, in radiative analyses is inadequate in the design and optimization of real materials. This is due to the strong influence on the phase function by the spectral optical properties and, to a lesser extent, the variation in the size parameter with wavelength.

Figures 6–8 show the spectral variation of the extinction $K_{e\lambda}$ and absorption $\sigma_{a\lambda}$ coefficients and the single scattering albedo $\sigma_{s\lambda}/K_{e\lambda}$ of the zirconia composite, respectively, for all fibers ($x_f = 1$), all spheres ($x_f = 0$), and a 50% mixture ($x_f = 0.5$) of both types of particles. It is reiterated that the diameter of the zirconia fibers ($r_f = 0.7$ μm) is about 10 times that of the spheres ($r_s = 0.075$ μm). The limited wavelength range is due to the lack of optical properties data for zirconia at longer wavelengths. This limited range still suffices for our

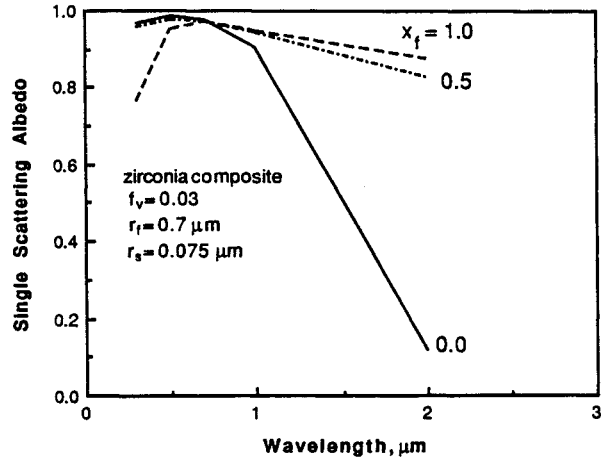

Fig. 8 Single scattering albedo of the zirconia composite for several fiber mixture fractions.

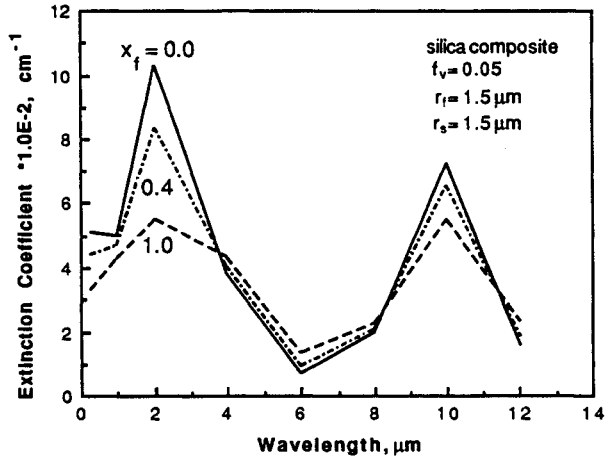

Fig. 9 Extinction coefficient of the silica composite for several fiber mixture fractions.

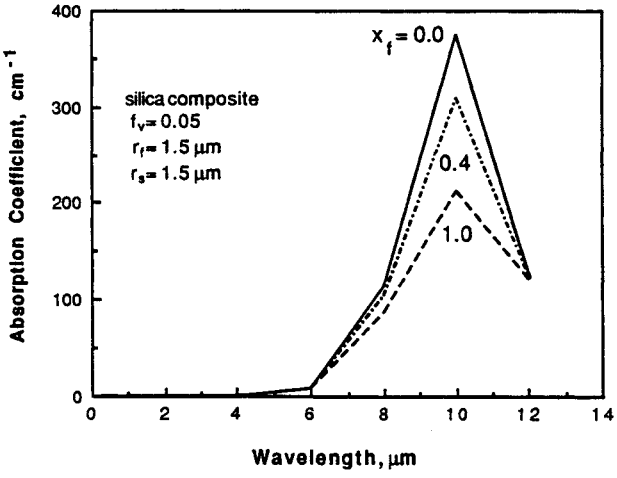

Fig. 10 Absorption coefficient of the silica composite for several fiber mixture fractions.

study, since we are examining the feasibility of increasing the uv surface reflectance of the composite. These results indicate that inclusion of spheres causes a substantial increase in the radiative properties in the uv, while the radiative properties are considerably reduced in the infrared. An increase in the scattering albedo reduces absorption, thus resulting in a higher surface reflectance, which is the desired trend.

The influence of composition on the radiative properties of silica composites is shown in Figs. 9–11. The silica fibers and spheres are of identical sizes ($r_f = r_s = 1.5$ μm), and mixture

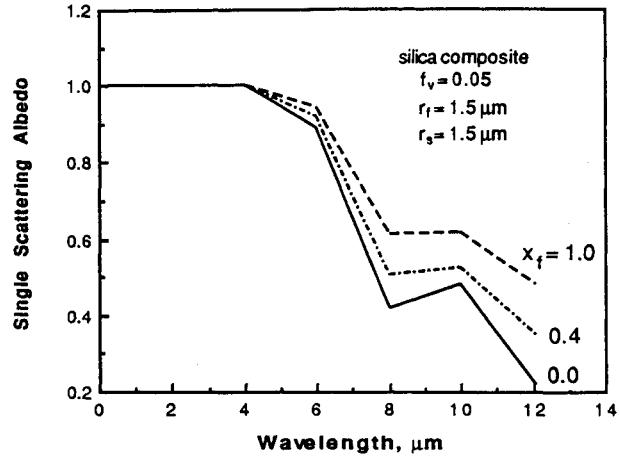

Fig. 11 Single scattering albedo of the silica composite for several fiber mixture fractions.

fractions of x_f = 0, 0.4, and 1 are considered. As shown in the figures, the presence of spheres increases the extinction coefficient at around $\lambda = 2$ μm, whereas the scattering albedo remains unchanged until $\lambda > 6$ μm. This is due to the extremely small absorption index of silica at $\lambda < 6$ μm, where the absorption coefficient is negligible. The surface reflectance at the shorter wavelength is expected to be quite high due to negligible absorption. At the longer wavelengths in the infrared, the presence of spheres reduces the scattering albedo, which then lowers the surface reflectance.

Examination of the results on the zirconia and silica composites reveals that sphere loading has a less pronounced effect on the silica composite than the zirconia composite due to the identical size parameters of the silica fibers and spheres. The results of the zirconia composite indicate that dissimilar fiber and sphere sizes allows greater flexibility in tailoring the radiative properties, and the results of the silica composite reveal the strong influence of optical properties. Therefore, optimization of the radiative properties of a fiber-sphere composite should exploit the influence of size and materials. The present results reveal that different materials and particle sizes should also be considered in the design of the fiber-sphere thermal insulation composites.

Summary

The present study examines the influence of materials and particle types on the radiative properties of a novel design of high-temperature, high-porosity thermal insulation composites consisting of spheres dispersed in a fibrous matrix. The analytical models for predicting the radiative properties of the composites are presented herein. Numerical analyses are conducted to examine the influence of relative loading of fibers and spheres on the extinction and absorption coefficients, the single scattering albedo, and the scattering phase function. The results reveal the strong influence of mixture ratio, optical properties, and size parameter on the radiative properties of the composite. Most importantly, these results demonstrate the feasibility of tailoring the radiative properties of the composite by dispersing spheres into the fibrous matrix. The present predictions will be verified by conducting optical extinction and scattering measurements on prototype materials.

Acknowledgment

This work was supported in part by NASA under SBIR Contract NAS2-13511.

References

[1]Page, W. A., Compton, D. L., Borucki, W. J., Ciffone, D. L., and Cooper, D. M., "Radiative Transport in Inviscid Nonadiabatic

Stagnation-Region Shock Layers," AIAA Paper 68-784, June 1968.

[2]Tauber, M. E., and Sutton, K., "Stagnation-Point Radiative Heating Relations for Earth and Mars Entry," *Journal of Spacecraft and Rockets*, Vol. 27, No. 4, 1990, pp. 40–42.

[3]Davy, S. C., Park, C., Arnold, J. O., and Balakrishnan, A., "Radiometer Experiment for the Aeroassist Flight Experiment," AIAA Paper 85-0967, June 1985.

[4]Howe, J. T., and Yang, L., "Earth Atmosphere Entry Thermal Protection by Radiation Backscattering Ablating Materials," *Journal of Thermophysics and Heat Transfer*, Vol. 7, No. 1, 1993, pp. 74–81.

[5]Stewart, D. A., Goldstein, H. E., and Leiser, D. B., "High Temperature Glass Thermal Control Structure and Coating," U.S. Patent 4381333, April 1983.

[6]White, S., "Reflective Overcoats for Thermal Control of Reentry Vehicles," AIAA Paper 91-1320, June 1991.

[7]Leiser, D. B., Churchward, R., Katvala, V., and Stewart, D. A., "Advanced Porous Coating for Low-Density Ceramic Insulation Materials," *Journal of the American Ceramic Society*, Vol. 72, No. 6, 1989, pp. 1003–1010.

[8]Van de Hulst, H. C., *Light Scattering by Small Particles*, Dover, New York, 1981.

[9]Kerker, M., *The Scattering of Light and Other Electromagnetic Radiation*, Academic Press, New York, 1969.

[10]Lee, S. C., "Radiation Heat Transfer Model for Fibers Oriented Parallel to Diffuse Boundaries," *Journal of Thermophysics and Heat Transfer*, Vol. 2, No. 4, 1988, pp. 303–308.

[11]Lee, S. C., "Effect of Fiber Orientation on Thermal Radiation in Fibrous Media," *International Journal of Heat and Mass Transfer*, Vol. 32, No. 2, 1989, pp. 311–319.

[12]Lee, S. C., "Scattering Phase Function for Fibrous Media," *International Journal of Heat and Mass Transfer*, Vol. 33, No. 10, 1990, pp. 2183–2190.

[13]Brewster, M. Q., and Tien, C. L., "Radiative Transfer in Packed Fluidized Beds: Dependent Versus Independent Scattering," *Journal of Heat Transfer*, Vol. 104, Nov. 1982, pp. 573–579.

[14]Lee, S. C., "Demarcation of Scattering Regimes in Fibrous Media," ASL Memorandum 199-60-01, July 1993.

[15]Krishna, M. G., Rao, K. N., and Mohan, S., "Optical and Structural Characterization of Evaporated Zirconia Films," *Applied Physics Letter*, Vol. 57, No. 6, 1990, pp. 557–559.

[16]Palik, E. D. (ed.), *Handbook of Optical Constants of Solids*, Academic Press, New York, pp. 753–761.

[17]White, S., Lee, S. C., and Grzesik, J. A., "Advanced Particulate Fibrous Composite for Thermal Control of Re-Entry Vehicles," AIAA Paper 93-2824, July 1993.